

strain is negligible. Because of the strain, the conformation of the intramolecular excimers of PC1, PC2, PC3, and PC4 may deviate from the sandwich geometry, which is the most stable conformation of an excimer.³⁴

Coops et al.⁴⁸ have measured the excess combustion enthalpies for various cycloalkanes. They found that 8-, 9-, 10-, and 11-membered rings have rather high strain energy, while larger cycloalkanes and cycloheptane have less strain, and cyclohexane has zero strain energy. The number of chain atoms of our samples, PC1, PC2, PC3, and PC4, is 7, 8, 9, and 10, respectively. The emission behavior of the strained excimer of our samples corresponds to the results of Coops et al., though the chains of our samples contain heteroatoms.

The dissociation rate of the excimer (k_d , Table IIIb) depends on chain length. At a given temperature, k_d becomes larger as the chain length decreases, which is clearly observed for PC1, PC2, PC3, and PC4. As mentioned above, PC1, PC2, PC3, and PC4 have a rather high strain of the chain when they are cyclized. The chain-length dependence of k_d shows that these excimers can easily dissociate because of the rather high strain of the cyclized chain. For the samples with $n \geq 6$, k_d gradually decreases with increasing chain length, while $\Delta\nu_e(\text{max}) = 0$. It seems that k_d is more sensitive to the strain of the cyclized chain than $\Delta\nu_e(\text{max})$. It should be noted that k_d is independent of chain length for sufficiently long chains^{16b} where cyclization does not induce strain energy.

The rate constant for the nonradiative process from the excimer (k_{nd} , Table IIIc) decreases as the chain length increases. This is also due to the instability of the excimer, which is brought about by the strain of the cyclized chain. However, the rate constant for the fluorescence from the excimer (k_{fd} , Table IIIc) is identical

for all samples. This may indicate that the emission process, whose rate is determined by the transition moment,⁴⁹ is less sensitive to the instability of the excimer than the nonradiative process.

Concluding Remarks

In the present work, it has been shown that the study of the intramolecular end-to-end excimer gives useful information on both dynamic behavior of the chain and the strain of the cyclized chain. As for the dynamic behavior, the intramolecular end-to-end collisional frequency was obtained as a function of the chain length and the temperature. The frequency, which corresponds to k_a , was proportional to the -1.5 power of the chain length in the temperature range above -60°C . The temperature dependence of k_a gave an apparent activation energy of ca. 5 kcal/mol for the intramolecular end-to-end excimer formation for all of the samples. This activation energy was analyzed in terms of Kramers' theory to evaluate the energy-barrier height for the conformational transition. The strain of the cyclized chain was evaluated by the emission properties of the intramolecular excimer. The wavelengths of the excimer emission peaks were blue shifted by about 15, 9, 5, and 3 nm for PC1, PC2, PC3, and PC4, respectively, at -60°C , since these compounds are highly strained in the cyclized state.

In the next paper, the ring-closure probability of the chain, which is governed by the conformational distribution in thermal equilibrium, will be discussed on the basis of intramolecular end-to-end excimer formation.

Registry No. PC0, 81496-96-0; PC1, 67512-97-4; PC2, 67512-98-5; PC3, 67512-99-6; PC4, 67513-00-2; PC6, 67513-01-3; PC8, 67513-02-4; PC10, 67513-03-5; PC14, 67513-04-6; PC18, 67513-05-7; PC22, 67513-06-8; MC4, 81478-03-7.

(48) Coops, J.; Kamp, H. van; Lambregts, W. A.; Wisser, J.; Decker, H. *Recl. Trav. Chim. Pays-Bas* **1960**, *79*, 1226.

(49) Mataga, N.; Kubota, T. "Molecular Interactions and Electronic Spectra"; Marcel Dekker: New York, 1970, Chapter 3.

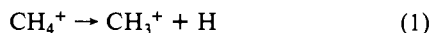
Fragmentation of Metastable CH_4^+ Ions and Isotopic Analogues. Kinetic Energy Release Distributions and Tunneling through a Rotational Barrier: Experiment and Theory

A. J. Illies, M. F. Jarrold, and M. T. Bowers*

Contribution from the Department of Chemistry, University of California, Santa Barbara, California 93106. Received October 13, 1981

Abstract: The fragmentation of metastable CH_4^+ , CD_3H^+ , and CD_4^+ ions has been studied with use of mass analyzed ion kinetic energy spectrometry (MIKES). Kinetic energy release distributions were derived from the MIKES peaks. The average kinetic energy release and metastable intensity were found to increase with ion source temperature. Appearance potential measurements indicated that the metastable reaction arises from CH_4^+ ions with internal energy close to the thermochemical threshold for fragmentation to give ground state $\text{CH}_3^+(^1\text{A}_1) + \text{H}(^2\text{S})$. The experimental data suggest that the origin of the metastable process is tunneling through a centrifugal barrier. A statistical model is presented and predictions of the model are compared with the experimental data.

The fragmentation of metastable CH_4^+ ions and its isotopic analogues via reaction 1 has been the subject of a number of



studies.¹⁻⁶ The principal reason for this interest is that the

observation of a metastable with a mass spectrometer requires a lifetime in the range 10^{-6} – 10^{-3} s, but statistical theories predict a lifetime in the nanosecond range for CH_4^+ . Hills et al.¹ attempted to reconcile the observation of the metastable by mod-

(1) L. P. Hills, M. L. Vestal, and J. H. Futrell, *J. Chem. Phys.*, **54**, 3834 (1971).

(2) C. E. Klots, *J. Phys. Chem.*, **75**, 1526 (1971).

(3) C. E. Klots, *Chem. Phys. Lett.*, **10** 422 (1971).

(4) B. H. Solka, J. H. Beynon, and R. G. Cooks, *J. Phys. Chem.*, **79** 859 (1975).

(5) V. H. Dibeler and H. M. Rosenstock, *J. Chem. Phys.*, **39**, 1326 (1963).

(6) J. P. Flamme, J. Momigny, and H. Wankenne, *J. Am. Chem. Soc.*, **98**, 1045 (1976).

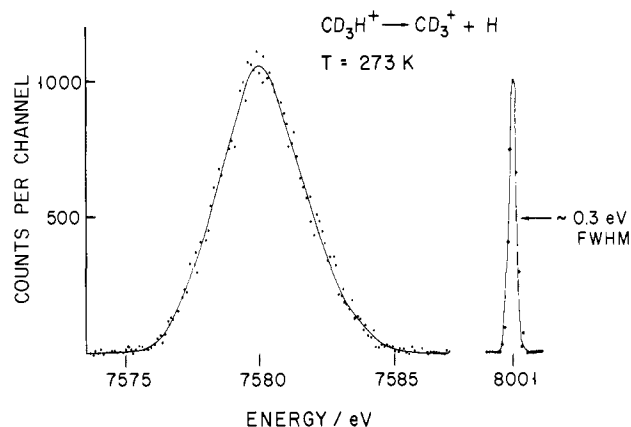


Figure 1. An example of the metastable and main beam MIKES peaks of CD_3H^+ measured at an ion source temperature of 273 K. The points are the data from the multichannel analyzer. The metastable peak was accumulated for approximately 30 min. The main beam peak was derived from several scans of the ESA and is arbitrarily normalized.

ifying the RRKM-QET theory to include the effects of reflection at a potential barrier. It appears likely, however, that a process other than vibrational predissociation is responsible for metastable reaction 1.² More recently Klots^{2,3} has suggested that the reaction is due to tunneling through a rotational barrier. Subsequently Solka, Beynon, and Cooks⁴ studied the reaction as a function of ion source temperature and found that the kinetic energy release (determined from the metastable peak width at half height) increased with temperature. This result was interpreted as being consistent with tunneling through a centrifugal barrier. However, these data could also be interpreted in terms of a slow electronic predissociation⁷⁻⁹ as originally suggested by Dibeler and Rosenstock.⁵ The CH_4^+ ion is Jahn-Teller distorted,^{10,11} and it is quite conceivable that a slow crossing between the states arising from the triply degenerate ${}^2\text{T}_2$ ground state could be responsible for the metastable process (see ref 10).

Flamme, Momigny, and Wankenne⁶ have measured the appearance potential of the metastable process. They found it to lie 1.7 eV above the appearance potential for fast CH_3^+ fragment ion production (i.e., CH_3^+ ions formed in the ion source at approximately the thermochemical threshold for reaction 1). This result differs from the earlier (1963) measurements of Dibeler and Rosenstock.⁵ They found that the fragment ion and metastable had the same appearance potential within 0.2 eV. Flamme et al. have interpreted their data as being consistent with tunneling through a rotational barrier. It is our opinion that their observation, if correct, can only reasonably be interpreted in terms of a curve-crossing mechanism.¹²

(7) The fragmentation of H_2S^+ ions provides an example of a metastable arising from a curve-crossing process. The kinetic energy release was found to increase with temperature (see ref 8). A forbidden electronic predissociation has been postulated for several reactions which show unusually small kinetic energy releases.⁹

(8) M. F. Jarrold, A. J. Illies, and M. T. Bowers, *Chem. Phys.*, **65**, 19 (1982).

(9) R. G. Cooks, K. C. Kim, and J. H. Beynon, *Chem. Phys. Lett.*, **26**, 131 (1974).

(10) R. N. Dixon, *Mol. Phys.*, **20**, 113 (1971).

(11) D. S. Gemmill, E. P. Kanter, and W. J. Pietsch, *J. Chem. Phys.*, **72**, 6818 (1980).

(12) The accuracy of the appearance potential measurement of Flamme et al.⁶ has been questioned by Stockbauer.¹³ However, at present we restrict discussion to the interpretation of these data. Flamme et al.⁶ suggest these measurements are consistent with tunneling through a rotational barrier. However, tunneling through a rotational barrier can only occur close to a dissociation threshold. The data of Flamme et al.⁶ might be interpreted in terms of tunneling through a rotational barrier in the fragmentation of an excited electronic state of CH_4^+ to give electronically excited products. However, there are no electronically excited states of the products in this energy range (1.7 eV above the ground state). Kari and Csizmadia¹⁴ have calculated the energy of the first excited state of CH_3^+ (on the assumption that it is planar) to be ~ 6.4 eV above the ground state. Hence we conclude that the only reasonable interpretation of the data of Flamme et al.⁶ is that it indicates that the metastable arises from a slow curve crossing.

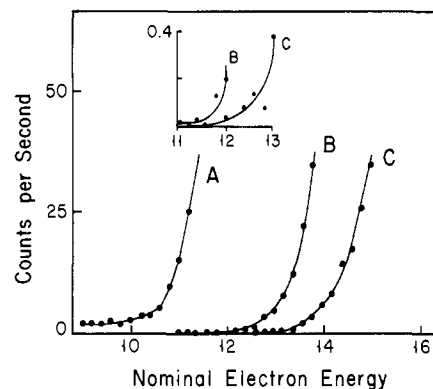


Figure 2. Ionization efficiency curves for CH_3^+ fragment ions formed in the ion source (A); CH_3^+ formed from metastable CH_4^+ in the second field free region (B); and CH_3^+ fragment ions formed in the ion source and normalized to the metastable count rate at 80 eV by closing the β slit (C).

From the above review it is clear that the origin of the metastable process has not been resolved. In this paper we report the results of a study of the metastable process with use of mass analyzed ion kinetic energy spectrometry (MIKES). We have remeasured the appearance potential of the metastable process and have measured the ratio of the metastable to main beam intensities as a function of temperature. Klots² has suggested that if the metastable is due to tunneling through a rotational barrier then the intensities should increase as T^2 . An increase in intensity of this magnitude would not be expected if the metastable arises from a curve-crossing process. (Compare ref 8.) These measurements thus provide an additional and perhaps more discriminating probe of the mechanism than the measurement of the kinetic energy release as a function of temperature alone. Further experiments were performed with a very high energy resolving power (approximately 25 000 fwhm). Kinetic energy release distributions were obtained from the resulting metastable MIKES peaks. A statistical model for the dissociation process is developed for tunneling through a centrifugal barrier. Results of calculations based on this model are compared with the experimental data.

Experimental Section

All measurements were performed with a reverse geometry mass spectrometer (VG Analytical, ZAB-2F) and a combined EI/CI temperature variable ion source constructed at UCSB (described in detail in a previous publication⁸). The ion source was operated under low-pressure electron-impact conditions with the accelerating voltage set at 8 kV and the electron energy set at 80 eV (except in the appearance potential measurements). The sample-gas pressure in the source was maintained so that the reading on the source ionization gauge was $3\text{--}4 \times 10^{-7}$ torr in all measurements reported here. Calibration of the ionization gauge with a capacitance manometer (MKS Baratron, Model 170M) indicated a source pressure of approximately 1×10^{-4} torr. At these source pressures the ions are extracted from the source under near collision free conditions. Experiments were performed with the isotopes CH_4 , CD_3H , and CD_4 (CH_4 : Matheson UHP 99.97%; CD_3H : Merck Sharp and Dohme 98% D_3 ; CD_4 : Stohler Isotope Chemicals 99% D). All gases were used without further purification.

Data were recorded with use of both analogue and digital data acquisition. The digital data acquisition system was similar to that described previously⁸ except for the addition of an Ortec 430 scaler. The appearance potential measurements were performed with pulse counting. Ion pulses were counted in the scaler for a predetermined time.

The ratio of the metastable to main beam intensities was determined from the ratio of the areas of the MIKES peaks. These data were recorded by using single scan analogue methods with the source slit open and collector slit closed until the intensity ratio was invariant with the collector slit setting.¹⁵

(13) R. Stockbauer, *Int. J. Mass. Spectrom. Ion Phys.*, **25**, 401 (1977).

(14) R. E. Kari and I. G. Csizmadia, *J. Chem. Phys.*, **46**, 1817 (1967).

Kinetic energy release distributions were derived from measurements of the metastable peak by using high energy resolving power (approximately 25 000 fwhm). The metastable peak was recorded with use of pulse counting techniques in a multichannel analyzer (as described in detail in ref 8). Figure 1 shows an example of the metastable and main beam MIKES peaks of CD_3H^+ measured at an ion source temperature of 273 K.

A possible source of error in the energy release measurements is the presence of a collision induced dissociation (CID) component in the metastable peak arising from ion-molecule collisions along the length of the second field free region and from within the collision cell. We believe the CID component is negligible in the data we present here.¹⁶ The pumping on the collision cell in the second field free region of the instrument has been improved and there was no detectable CID arising from within the cell. The indicated analyzer pressure was less than 4×10^{-9} torr.

Results

a. Appearance Potential. Figure 2 shows the results of the appearance potential measurements. Curve A is the ionization efficiency curve for the CH_3^+ fragment ion formed in the ion source, and curve B is the ionization efficiency curve for CH_3^+ formed from metastable CH_4^+ in the second field free region of the mass spectrometer. The apparent appearance potentials are significantly different. These results are similar to those of Flamme et al.⁶ Curve C is the ionization efficiency curve for fragment ion CH_3^+ formed in the ion source normalized to the metastable count rate at 80 eV by closing the β slit (between the magnet and ESA). Note that by reducing the CH_3^+ intensity (by a factor of approximately 10^5) the apparent appearance potential is shifted in energy by approximately 2–3 eV.

The likely origin of this shift in apparent appearance potential is the Maxwell-Boltzmann distribution of electron energies from the filament. If $\sigma(E)$ is electron impact ionization cross section at electron energy E , the measured intensity $I(E')$ is given by¹⁷

$$I(E') = c \int \sigma(E)f(E) dE \quad (2)$$

where $f(E)$ is the electron energy distribution. The measured appearance potential occurs at a nominal electron energy E' when $I(E')$ is greater than the detection threshold. (This, for example, could be the detection of one ion count in a predetermined period of time.) Electrons leaving the filament have a Maxwell-Boltzmann energy distribution given by¹⁸

$$dN(\epsilon)/d\epsilon = \epsilon \exp(-(\phi + \epsilon)/kT) \quad (3)$$

where ϕ is the work function and ϵ the thermal energy of the electron. This distribution peaks within a few tenths of an electron volt but has a tail which falls off exponentially, extending for several electron volts. It is apparent from this distribution that by reducing the detection threshold by a factor of 10^5 (this is the

(15) The metastable to main beam intensity ratio was found to vary with source and collector slit settings. The method of choice for measuring intensities is with the slits open. This produces flat top peaks and the intensity is proportional to the height. However, in addition to Y (and Z) discrimination, the off-axis configuration of the multiplier in the ZAB-2F introduces energy discrimination into the MIKES scan producing peaks which are not flat topped. This makes it difficult to determine the intensities from the peak heights with confidence. Closing the collector slit produces a triangular peak shape. The intensity is then proportional to the area of the peak. The apparent metastable to main beam intensity ratio (derived from the peak areas) was found to increase to a limiting value as the collector slit was further closed. Closing the source slit then reduced the intensity ratio. These variations of the intensity ratio with slit settings are presumably due to the different energy distributions of the metastable and main beams. The true intensity ratio will be determined when the resolution of the energy analyzer is small compared with the apparent energy distributions of the metastable and main beams. Closing the collector slit increases the resolving power, thus the intensity ratio increases to a limiting value which represents the true intensity ratio. Closing the source slit will reduce the angular dispersion of the main beam, reducing the apparent energy distribution and thus reducing the intensity ratio.

(16) The relative intensities of the CID and metastable components vary with temperature and isotopic variant. For CD_3H^+ at 500 K the CID peak intensity ($I(E) dE$) is estimated to be approximately 0.3% of the peak metastable intensity.

(17) C. E. Melton, "Principles of Mass Spectrometry and Negative Ions", Marcel Dekker, New York, 1970.

(18) J. B. Hasted, "Physics of Atomic Collisions", Butterworths, London, 1964.

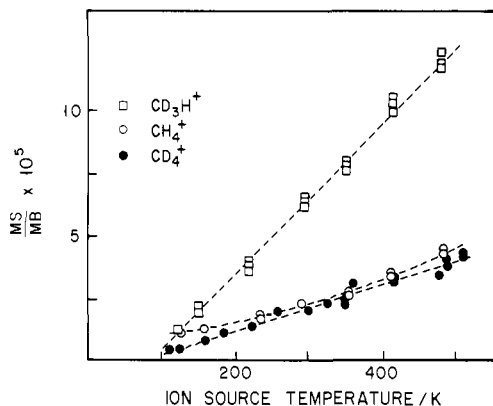


Figure 3. A plot of the relative metastable to main beam intensity ratios against ion source temperature for the fragmentation of CH_4^+ (O), CD_3H^+ (□), and CD_4^+ (●).

effect of closing the β slit) the measured appearance potential may be shifted to higher energy by several electron volts, as we have observed.

Since the metastable intensity is approximately 10^5 times smaller than the fragment ion intensity, we would expect the measured appearance potential for the metastable to be shifted to a higher energy than the fragment ion, even if the true appearance potentials were the same. When the CH_3^+ intensity is normalized to the metastable intensity at 80 eV, the measured appearance potentials are much closer (see the insert in Figure 2). From these data we conclude that the true appearance potentials of the metastable and fragment ion are the same within a few tenths of an electron volt. More quantitative conclusions are not possible from these data since the ionization efficiency curves for the two processes have significantly different shapes. These results are in agreement with the findings of Dibeler and Rosenstock.⁵ They concluded that the appearance potentials of the metastable and CH_3^+ fragment ion were the same within 0.2 eV. The incorrect conclusions made by Flamme et al.⁶ about the appearance potential of the metastable process relative to the direct process appear to be due to the Maxwell-Boltzmann distribution of electron energies from the filament and the fact that the intensity of the fragment ion is approximately 10^5 times greater than that of the metastable.¹⁹

b. Intensities. Intensity measurements were made over the ion source temperature range 100–500 K for the isotopes CH_4^+ , CD_4^+ , and CD_3H^+ . Figure 3 shows plots of the intensities against temperature. For the fragmentation of CD_3H^+ only the H loss process was observed (indicating that H loss is >100 times more intense than the D loss process). The preferential loss of H rather than D has been observed previously²¹ and has been explained by Hills et al.¹ as being due to zero-point energy effects. The H loss process is approximately 80 meV lower in energy than D loss.

From Figure 3 it is apparent that the intensities of the metastables from CH_4^+ and CD_4^+ are very similar over the temperature range. The intensity from CD_3H^+ is substantially greater for $T > 150$ K. The metastable intensity for all three reactions increases as the ion source temperature is raised. However, the intensities do not increase as T^2 as predicted by the model of Klots² for tunneling through a centrifugal barrier. This point will be discussed in more detail below.

(19) A few additional comments are useful here. Although the measurement of appearance potentials with use of a conventional EI source is far from the method of choice, it is relatively easy and an extensive literature²⁰ exists on the optimum procedures to employ. The measurement of appearance potentials of metastable ions is particularly difficult, and the significance of the values obtained is questionable. These measurements should be performed on an instrument designed specifically for this purpose. If, however, these measurements must be performed with use of a conventional EI source, particular attention must be given to instrumental effects.

(20) J. H. Beynon, R. G. Cooks, K. R. Jennings, and A. J. Ferrer Correia, *Int. J. Mass. Spectrom. Ion Phys.*, **18**, 87 (1975); R. K. Boyd and J. H. Beynon, *ibid.*, **23**, 163 (1977).

(21) Ch. Ottinger, *Z. Naturforsch.*, **A**, **20A**, 1232 (1965).

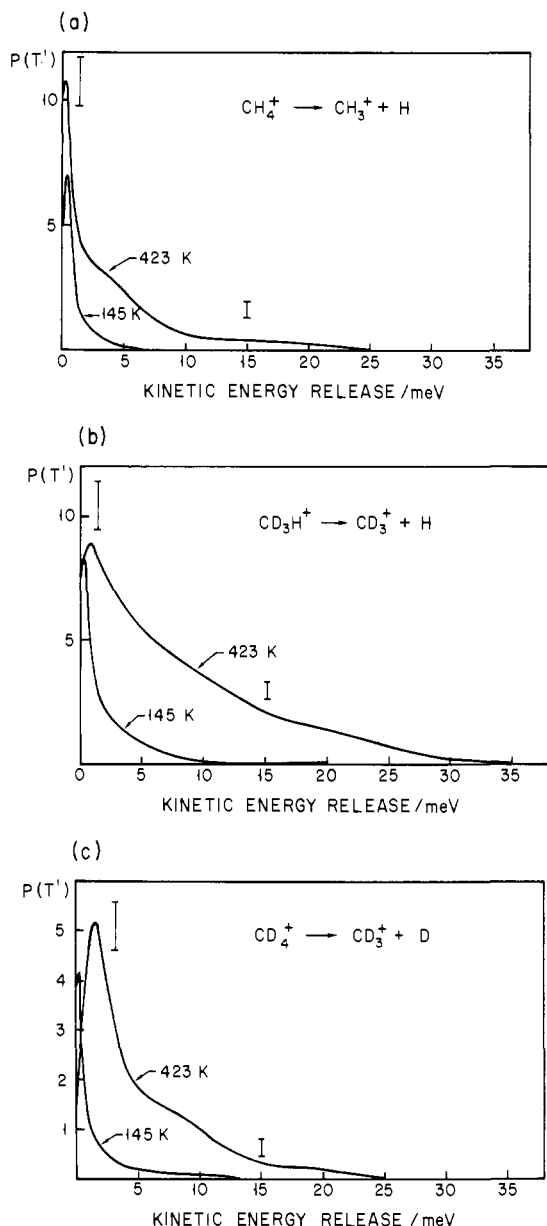


Figure 4. Kinetic energy release distributions for the fragmentation of metastable CH_4^+ (a), CD_3H^+ (b), and CD_4^+ (c) at ion source temperatures of 145 and 423 K. Estimated error bars are shown. For normalization procedure see text.

c. Kinetic Energy Release. Kinetic energy release distributions have been derived from the measurements of the metastable MIKES peak with use of high energy resolving power (approximately 25 000 fwhm). Figure 1 shows an example of the metastable and main beam MIKES peaks. The main beam is much narrower than the metastable. The kinetic energy release distributions can thus be determined directly from the metastable peak without making corrections for the main beam energy width. The distributions were determined by drawing a smooth curve through the metastable MIKES points followed by numerical differentiation.²²

Figure 4 shows the kinetic energy release distributions for the fragmentation of CH_4^+ , CD_3H^+ , and CD_4^+ at ion source tem-

(22) The equation for the derivation of the kinetic energy release distribution from the metastable MIKES peak is²³

$$P(T') dT' = dI/dE$$

where $P(T') dT'$ is the center of mass kinetic energy release distribution and dI/dE is the derivative of the MIKES peak in LAB energy space.

(23) J. L. Holmes and A. D. Osborne, *Int. J. Mass. Spectrom. Ion Phys.*, **23**, 189 (1977).

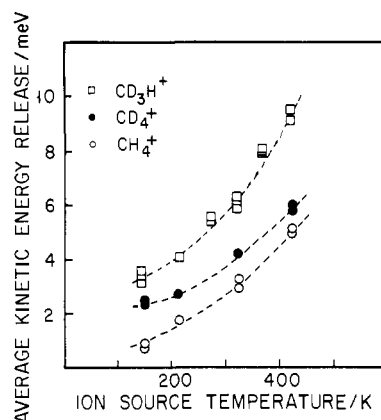


Figure 5. A plot of the average kinetic energy release, derived from the distributions, against temperature for the fragmentation of metastable CH_4^+ (○), CD_3H^+ (□), and CD_4^+ (●).

peratures of 145 and 423 K. The distributions have been normalized so that the total intensity given by $\int P(T) dT$ equals the experimental intensities given in Figure 3. Note that as the temperature is raised the distributions become much broader. At high temperature the distributions for CD_4^+ and CH_4^+ are much narrower than the CD_3H^+ distribution. At low temperature the distributions appear more similar.

Figure 5 shows a plot of the average kinetic energy release, derived from the distributions, against temperature. The average energy release increases substantially with temperature for all three isotopic analogues. The average releases for CH_4^+ and CD_4^+ fragmentation are fairly similar except at low temperature. The average release for CD_3H^+ fragmentation shows the largest temperature dependence.

Theory

The intensity and appearance potential measurements are consistent with the hypothesis that the metastable arises from tunneling through a centrifugal barrier close to the thermochemical threshold for fragmentation to ground state $\text{CH}_3^+(^1A_1) + \text{H}(^2S)$.²⁴ We will now derive a statistical model for the tunneling process to test this hypothesis and as an aid to understanding and interpreting the trends evident in the data.

Until recently little attention was paid to the inclusion of the effects of tunneling into statistical theories of unimolecular reactions. However, in a recent series of papers Miller and co-workers²⁵⁻²⁸ have considered the effects of tunneling in unimolecular reactions in some detail. In particular they have investigated tunneling through a configurational barrier in the unimolecular decomposition of formaldehyde^{25,26} and the isomerization of vinylidene.²⁷ Klots³ has briefly considered the problem of tunneling through a centrifugal barrier for CH_4^+ and CD_4^+ . Flamme and Momigny²⁹ have also considered tunneling through a centrifugal barrier, but they do not treat the problem from within a statistical framework.³⁰

(24) Varying the temperature over the range 100–500 K does affect the vibrational distribution of the neutral. This may result in a change in the vibrational distribution of the ion. However, CH_4 is predominantly in the ground vibrational level over the temperature range and the Frank-Condon manifold of CH_4^+ is broad, hence we expect changes in the CH_4^+ vibrational distribution in the metastable energy range to be small. Thus we presume the changes in kinetic energy release and metastable intensity are due to changes in the rotational distribution of the neutral which we expect to be carried through to the ion.

(25) W. H. Miller, *J. Am. Chem. Soc.*, **101**, 6810 (1979).

(26) S. K. Gray, W. H. Miller, Y. Yamaguchi, and H. F. Schaefer, III, *J. Am. Chem. Soc.*, **103**, 1900 (1981).

(27) Y. Osamura, H. F. Schaefer, III, S. K. Gray, and W. H. Miller, *J. Am. Chem. Soc.*, **103**, 1904 (1981).

(28) B. A. Waite and W. H. Miller, *J. Chem. Phys.*, **73**, 3713 (1980).

(29) J. P. Flamme and J. Momigny, *Chem. Phys.*, **34**, 303 (1978).

(30) Flamme and Momigny²⁹ treat the dissociation as quasidiatomic. They argue that statistical theories will not be valid for an ion as small as CH_4^+ . On the contrary, for metastable CH_4^+ ions it is our belief that statistical theory is a reasonable framework due to the long lifetime of the ions and the fact that they occupy the ground electronic state.

Here we will consider the problem of tunneling through a centrifugal barrier from within a statistical framework and calculate microscopic rate constants (E, J_0) from which kinetic energy release distributions and metastable intensities can be calculated for comparison with experiment. Our basic philosophy is to use the simplest realistic model available which we will test against the data and subsequently use as an aid to understanding and interpreting the trends evident in the data. Noting that the centrifugal barrier occurs at relatively large CH_3^+-H separations, we consider the fragmentation to occur as follows. The vibrationally excited CH_3^+ and H moieties begin to separate. When the centrifugal barrier is encountered there is a finite probability that tunneling will occur through the barrier and the products separate to $r = \infty$. If tunneling does not occur then the incipient products are reflected at the barrier. The CH_3^+ and H moieties recombine and redistribute their vibrational energy until they again begin to separate. The rate constant for tunneling through a barrier characterized by an orbital angular momentum L at energy E is then given by

$$k(E, L) = \omega(E, J_0) P(T', L) \quad (4)$$

where $\omega(E, J_0)$ is the number of times the barrier is encountered per second, $P(T', L)$ is the tunneling probability for one-dimensional motion along the reaction coordinate, J_0 is the total angular momentum, and T' is the kinetic energy release, given by

$$T' = E - E_0 - \epsilon_R(J, K) \quad (5)$$

where E_0 is the reaction endoergicity and $\epsilon_R(J, K)$ is the product rotational energy. The frequency of barrier encounter $\omega(E, J_0)$ is derived from statistical theory. For energies below the classical reaction threshold only the ground state of the transition state contributes to the frequency factor^{25,27} and $\omega(E, J_0)$ is given by

$$\omega(E, J_0) = (\hbar \rho(E, J_0))^{-1} \quad (6)$$

where $\rho(E, J_0)$ is the density of states³¹ of the reactant ion in its equilibrium configuration. The $P(T', L)$ term is evaluated with the WKB approximation^{38,39} and is given by

$$P(T', L) \approx \exp \left[-\frac{2}{\hbar} \int_{r_1}^{r_2} [2\mu \{V(r, L, J) - T' - \epsilon_R(J, K)\}]^{1/2} dr \right] \quad (7)$$

where the integral is evaluated over the width of the barrier $r_2 - r_1$. The WKB approximation fails in the region of the top of the barrier. However, tunneling from near the top of the barrier does not contribute to the metastable intensity detected in our instrument. The effective potential function $V(r, L, J)$, is given by

$$V(r, L, J) = -\frac{q^2 \alpha_H}{8\pi \epsilon_0 r^4} + \frac{L^2 \hbar^2}{2\mu r^2} + \epsilon_R(J, K) \quad (8)$$

where α_H is the polarizability of the H atom, q is the charge on the electron, μ is the reduced mass, and ϵ_0 is the permittivity of free space. The first term represents the attractive ion-induced dipole potential and the second term is the repulsive rotational contribution arising from the orbital angular momentum.

The unimolecular rate constant, $k(E, J_0)$, for the tunneling of an ion with internal energy E and angular momentum J_0 is evaluated by summing eq 4 over the available product angular momentum states (J, L). Thus⁴⁰

$$k(E, J_0) = \sigma \omega(E, J_0) \sum_L \sum_J \sum_K P(T', L) \quad (9)$$

where σ is a symmetry factor. Conservation of angular momentum requires

$$\vec{J}_0 = \vec{J} + \vec{L} \quad (10)$$

where \vec{J}_0 is the reactant ion angular momentum and \vec{J} and \vec{L} are the rotational and orbital angular momenta of the products, respectively.

We must now address the question of how the available angular momentum is partitioned between J and L . A question that must be answered is: are there any dynamic constraints or is a statistical treatment valid? Chupka⁴¹ and McCulloh and Dibeler⁴² have conducted detailed photonionization efficiency studies of reaction 1 and found that the full rotational energy is available to drive the reaction close to threshold, i.e., energy (and hence angular momentum) is not constrained to remain in the rotor about the symmetry axis of the transition state. This circumstance must also occur for the tunneling reaction. Thus, there appear to be no dynamic constraints on the partitioning of the angular momentum and the available angular momentum phase space is given by

$$L = J_0 + J, \dots, |J_0 - J|; \quad J = J_0 + L, \dots, |J_0 - L| \quad (11)$$

restricted by the energetic constraint

$$\epsilon_R(J, K) < E - E_0 \quad (12)$$

Finally, to be rigorous, we put an energetic constraint on eq 9

$$E - E_0 < E_m(J_0) \quad (13)$$

where $E_m(J_0)$ is the minimum energy at which the reaction can occur classically.⁴³ Above this energy the reaction can occur both classically and by tunneling, while below this energy the reaction can occur only by tunneling. For those angular momentum states for which the reaction proceeds classically, the tunneling probability $P(T', L) = 1$ and must be multiplied by the sum of vibrational states at the transition state, $N^{\ddagger}(E_v)$. For those angular momentum states for which the reaction proceeds by tunneling, only the ground vibrational state of the transition state contributes. Thus,

(40) Writing eq 9 in its more explicit form

$$k(E, J_0) = \frac{\sigma \sum_L \sum_J \sum_K P(T', L)}{\hbar \rho(E, J_0)}$$

permits comparison with the standard RRKM expression

$$k(E, J_0) = \frac{\sigma N^{\ddagger}(E, J)}{\hbar \rho(E, J_0)}$$

This demonstrates the difference between the two expressions; that is, $N^{\ddagger}(E, J)$, the sum of states at the transition state, is replaced by $\sum_L \sum_J \sum_K P(T', L)$, the sum of the tunneling probabilities. (Compare ref 25 and 27).

(41) W. A. Chupka, *J. Chem. Phys.*, **48**, 2337 (1968).

(42) K. E. McCulloh and V. H. Dibeler, *J. Chem. Phys.*, **64**, 4445 (1976).

(43) $E_m(J_0)$ corresponds to the minimum energy at which the reaction can occur classically. If $B(L)$ is the height of the centrifugal barrier with orbital angular momentum L , then $E_m(J_0)$ is given by the minimum value of $B(L) + \epsilon_R(J, K)$ with $J_0 = L + J$.

(31) The density of states $\rho(E, J_0)$ is given by³²

$$\rho(E, J_0) = (2J_0 + 1) \rho(E - E_R)$$

The vibrational density of states $\rho(E - E_R)$ was calculated with the Whitten-Rabinovich approximation.³³ The vibrational frequencies employed were derived from the vibrations of the neutral molecules³⁴ and those vibrations observed in the photoelectron spectrum of CH_4 .³⁵ The rotational constants employed were those of the neutral molecules.^{36,37}

(32) For discussion, see: W. J. Chesnavich and M. T. Bowers in "Gas Phase Ion Chemistry", Vol. 1, M. T. Bowers, Ed., Academic Press, New York, 1979.

(33) For a discussion, see: P. J. Robinson and K. A. Holbrook, "Unimolecular Reactions", Wiley-Interscience, London, 1972.

(34) G. Herzberg, "Infra-Red and Raman Spectra", Van Nostrand, New York, 1960.

(35) A. W. Potts and W. C. Price, *Proc. R. Soc. London, Ser. A*, **A326**, 165 (1972).

(36) G. Herzberg, "Electronic Spectra of Polyatomic Molecules", Van Nostrand, New York, 1966.

(37) G. Herzberg, *Proc. R. Soc. London, Ser. A*, **A262**, 291 (1961).

(38) D. Bohm, "Quantum Theory", Prentice Hall, New York, 1966.

(39) L. D. Landau and E. M. Lifshitz, "Quantum Mechanics: Non-Relativistic Theory", Pergamon, New York, 1977.

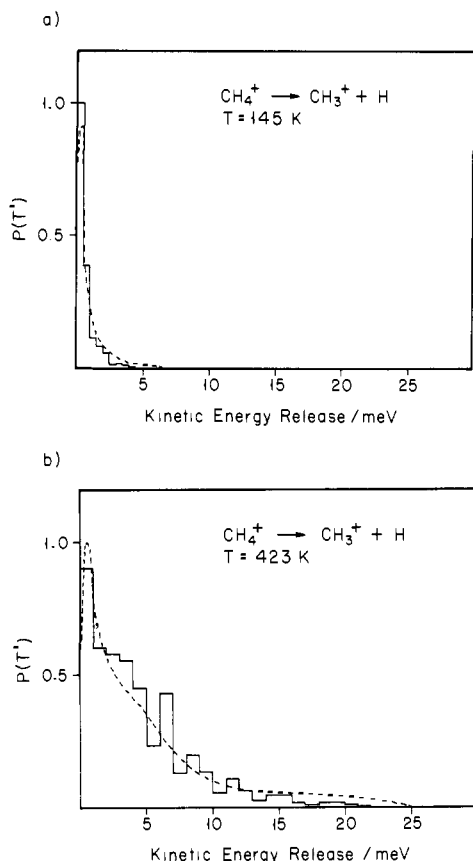


Figure 6. A comparison between the experimental (---) and calculated (histogram) kinetic energy release distributions for the fragmentation of CH_4^+ at ion source temperatures of 145 K (a) and 423 K (b). The experimental and calculated distributions have been normalized to the same total intensity.

$N^z(E_v) = 1$ and must be multiplied by the tunneling probability. Hence, in general

$$k(E, J_0) = \frac{\sigma \sum_L \sum_J \sum_K P(T', L) N^z(E_v)}{h\rho(E, J_0)} \quad (14)$$

which is a statement of the RRKM equation which includes the effects of tunneling through a rotational barrier.

Trial calculations indicate that for the metastable reaction $k(E, J_0)$ can be approximated to

$$k(E, J_0) = \sigma \omega(E, J_0) \sum_L P(T', L) \quad (15)$$

$$L = J_0 - J; \quad \epsilon_R(J, K) < E - E_0$$

without introducing any significant error. The sum over K can be neglected because tunneling occurs predominantly to produce CH_3^+ in the lowest level of the K manifold. The double sum over L and J can be replaced by a sum over L with $L = J_0 - J$ because tunneling to produce CH_3^+ with angular momentum J occurs predominantly through the barrier with the smallest L allowed by conservation of angular momentum.⁴⁴ This approximation introduces less than 1% error yet considerably shortens the computation time.

The kinetic energy release distribution was evaluated as follows. For given E and J_0 the fraction of ions fragmenting with kinetic energy release T' in the time window sampled in the experiment, $F(T')_{E, J_0}$ was determined from

$$F(T')_{E, J_0} = \frac{k(T', L)}{k(E, J_0)} [e^{-k(E, J_0)t_1} - e^{-k(E, J_0)t_2}] \quad (16)$$

where t_1 and t_2 define the time window sampled in the experi-

(44) Thus tunneling occurs predominantly for the states in which \vec{J} and \vec{L} are aligned parallel.

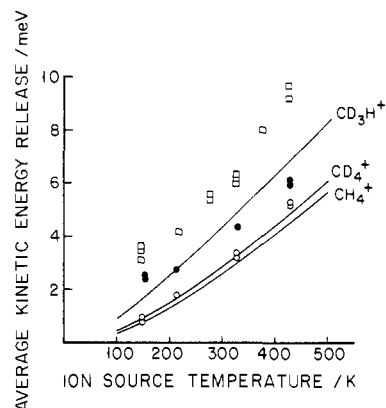


Figure 7. A plot of the average kinetic energy releases against ion source temperature: experiment (CH_4^+ (O), CD_3H^+ (□), CD_4^+ (●)) and calculated (—).

ment.⁴⁵ This fraction was then summed over all internal energies E for which tunneling occurs in the metastable time range and convoluted with the reactant rotational distribution. Thus

$$P(T') dT' = \sum_{J_0} \sum_E P(E) P(J_0) F(T')_{E, J_0} \quad (17)$$

where $P(E)$ ⁴⁶ and $P(J_0)$ ⁴⁷ are the probabilities of forming the ion with internal energy E and angular momentum J_0 , respectively. The average kinetic energy release and total intensity were then derived from the distributions.

Figure 6 shows a comparison between the calculated and experimental kinetic energy release distributions for the fragmentation of CH_4^+ at ion source temperatures of 145 and 423 K, respectively. There is good agreement between the theoretical predictions and experiment. The agreement between the theory and experiment for CD_4^+ and CD_3H^+ is of about the same quality. The oscillations evident in the high-temperature theoretical distribution in Figure 6 are due to the fact that for an ion with angular momentum J_0 tunneling in the metastable time window occurs over a relatively narrow range of internal energies and hence produces products with a relatively narrow range of kinetic energies. There is no evidence for this structure in the experimental distribution. This structure if present would not be detectable in our data because of the noise and relatively low energy resolution in the center of mass frame. However, Flamme et al.⁴⁸ have observed structure in the metastable peaks for CH_4^+ and CD_4^+ by using a monoplasmatron ion source which has a much higher working temperature ($\sim 1500 \text{ K}$).

Figure 7 shows plots of the average kinetic energy release predicted by the theory against temperature for all three isotopic analogues. The experimental data are also shown for comparison. The agreement between theory and experiment is reasonably good. The trends predicted by the theory are certainly in agreement with the experiment, although the calculated average releases are consistently smaller than the experimental values. Such disagreement would be expected if the centrifugal barrier is larger than predicted by the Langevin model (i.e., the potential surface is less attractive than the ion-induced dipole potential). Powis⁴⁹ has performed photoion-photoelectron coincidence measurements and phase space calculations on reaction 1 for energies near

(45) We assume an ion source residence time of $2 \mu\text{s}$. Varying this parameter over the range $0-4 \mu\text{s}$ was found to have only a small effect on the average kinetic energy release. Although the intensities were more sensitive, they were found to scale with the residence time.

(46) We assume a continuum of vibrational levels behind the barrier. This is a reasonable assumption as the vibrational densities of states are in the range $50-500 \text{ meV}^{-1}$. We further assume $P(E) dE = 1$. This is valid because tunneling occurs over such a small energy range.

(47) We assume the rotational distribution of the ion is given by the neutral thermal distribution (compare ref 41 and 42). The effects of nuclear symmetry on the degeneracy of the rotational levels were neglected since these effects will be scrambled to a large extent in the ionization process.

(48) J. P. Flamme, H. Wankenne, R. Loch, J. Momigny, P. J. C. M. Nowak, and J. Los, *Chem. Phys.*, **27**, 45 (1978).

(49) I. Powis, *J. Chem. Soc., Faraday Trans. 2*, **75**, 1293 (1979).

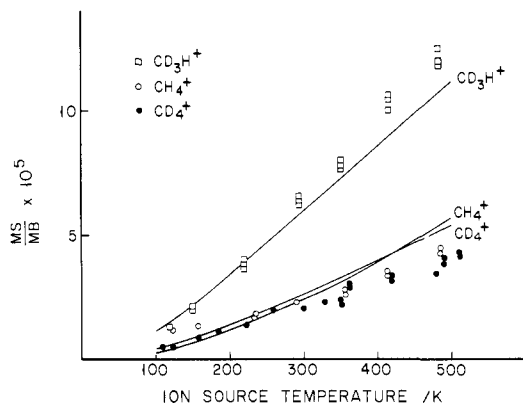


Figure 8. A plot of the metastable to main beam intensity ratios against ion source temperature: experiment (CH_4^+ (○), CD_3H^+ (□), CD_4^+ (●)) and calculated (—).

threshold. He also found that the phase space calculations did not give exact quantitative agreement with the experimental results and suggested that this discrepancy may be due to the underestimation of the height of the centrifugal barrier by the Langevin model.

Figure 8 shows a plot of the calculated and experimental intensities against temperature. Absolute intensities were not calculated so the calculated data have been scaled to give the best overall fit with the experimental data. The trends predicted by the theory are in good agreement with the experimental results. Note in particular that the intensities predicted for CH_4^+ and CD_4^+ fragmentation are similar and substantially less than the CD_3H^+ metastable intensity as is observed in the experimental results and that the intensities are predicted to increase nearly linearly with temperature in agreement with the data.

Discussion

The agreement between the experimental results and the predictions of the tunneling model is remarkably good. The model predicts a substantial increase in intensity and kinetic energy release as the temperature is raised. The increase in kinetic energy release arises because, as the temperature is raised, higher J_0 levels are populated, the centrifugal barrier is higher, and tunneling occurs at higher energy above threshold. Klots² correctly predicted an increase in metastable intensity with temperature but for apparently the wrong reasons. His basic assumption was the average height of the centrifugal barrier, and hence what he termed the "tunneling width" increased with the thermal rotational energy squared and hence as T^2 . He suggested that this would result in the metastable intensity increasing as T^2 . However, if we note that the metastable intensity arises from a narrow window on the centrifugal barrier, the origin of the increase in intensity is not immediately obvious. The tunneling model provides an elegant explanation for the increase in intensity. As the orbital angular momentum is raised, the barrier changes shape from low and wide to high and narrow. This change in shape results in an increase in the size of the metastable tunneling window, as shown in Figure 9, and hence an increase in metastable intensity. It should be noted with regard to Figure 9 that tunneling in the metastable range from the higher J_0 levels does not occur predominantly through the barrier with $L = J_0$ but through smaller barriers to produce rotationally excited CH_3^+ . For example, for CH_4^+ ($J_0 = 14$) tunneling occurs predominantly to produce CH_3^+ ($J = 1$) and significant amounts of CH_3^+ ($J = 2$ and 3).

The agreement between the model and experiment suggests that the differences between the intensities and kinetic energy releases for the various isotopic species arise from a number of factors: (1) lower effective barriers for CH_4^+ and CD_4^+ fragmentation, since tunneling will occur through the lowest of the four available barriers; (2) the frequency of barrier encounter $\omega(E, J_0)$ which is dependent on the density of states and increases in the order $\text{CD}_4^+ < \text{CD}_3\text{H}^+ < \text{CH}_4^+$; and (3) the barrier height which is dependent on the reduced mass and varies in the order $\text{CH}_4^+ \approx \text{CD}_3\text{H}^+ > \text{CD}_4^+$. Other factors such as differences in the rota-

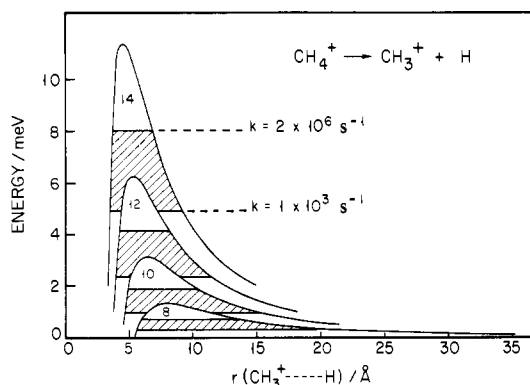


Figure 9. Variation of position and size of metastable tunneling window with orbital angular momentum. Barriers are shown for $L = 8, 10, 12,$ and 14 with $J = 0$. The shaded areas on the barriers show the size of the metastable tunneling windows (rate constants in the range $(2 \times 10^6) - (1 \times 10^3) \text{ s}^{-1}$).

tional energy levels for CH_3^+ and CD_3^+ and the symmetry of the reactant ion are also important, but we believe the factors itemized above are the most significant. Thus, the kinetic energy releases and intensities for CD_4^+ are lower than those for CD_3H^+ fragmentation mainly because of the lower centrifugal barriers for CD_4^+ (resulting from the larger reduced mass). The differences between the results for CD_3H^+ and CH_4^+ fragmentation are due mainly to the much faster rate of barrier encounter in CH_4^+ (resulting in the metastable tunneling window being lower down the barrier and smaller) and that fact that the distribution of J levels populated in CH_4^+ is lower than in CD_3H^+ , leading to lower centrifugal barriers for CH_4^+ . Thus the similarity between the results for CH_4^+ and CD_4^+ fragmentation is "accidental" and arises from the interplay of a number of factors.

A few additional comments are required with regard to the sensitivity of the tunneling mechanism to mass. It has been suggested on several occasions that the tunneling mechanism is insensitive to mass.^{3,4} The effects of mass can be seen by comparison of the results for CD_3H^+ and CD_4^+ (not CH_4^+ and CD_4^+). The metastable intensity from CD_3H^+ fragmentation is approximately twice the CD_4^+ intensity. This is not due to the usual mass dependence of tunneling (D atom emission is actually more facile for a given barrier height³). The smaller intensity for CD_4^+ fragmentation is due mainly to the smaller centrifugal barriers for D atom loss leading to smaller metastable windows as noted above.

Conclusions

The appearance potential and intensity data both suggest that the metastable reaction arises from tunneling through a rotational barrier. The good agreement between the experimental data and the predictions of the tunneling model supports this hypothesis. The increase in kinetic energy release with temperature arises because higher J_0 levels are populated, the centrifugal barrier is higher, and tunneling occurs at a higher energy above threshold. The metastable to main beam intensity ratio increases with the ion source temperature because the size of the metastable tunneling window increases with increasing J_0 . The model provides a rationale for the trends evident in the data for the series CH_4^+ , CD_3H^+ , and CD_4^+ . The differences between the intensities and kinetic energy release arise from the interplay of a number of factors.

Further experiments, on other reactions, and the development of a more rigorous theoretical treatment are currently in progress.

Acknowledgment. We gratefully acknowledge the support of the National Science Foundation under Grant CHE80-20464. M.F.J. also acknowledges the Science Research Council (UK) for a NATO/SRC fellowship. It is a pleasure to acknowledge a number of stimulating discussions with Dr. Lew Bass.

Registry No. CH_4^+ , 20741-88-2; CD_4^+ , 34510-07-1; CD_3H^+ , 61105-68-8.